The Journal of Materials Chemistry

Microscopic vs macroscopic structural evolution of SiO_2 sols and gels employing a tailor-made fluorescent reporter dye

Brita Unger, Knut Rurack, Ralf Müller, Harald Jancke and Ute Resch-Genger

Electronic Supplementary Information

S1 Correction of fluorescence spectra. Fluorescence spectra obtained for TEOS-derived sols and gels can be strongly distorted by Raman scattering from the matrix. To account for this problem, we investigated a series of undoped samples prepared and treated in the same way as the dye-doped samples. Additionally, measurements with crossed polarizers were performed. After background subtraction, all the spectra were corrected for the spectral responsivity of the instrument. To minimize potential errors from residual background signals, every corrected spectrum was fitted to a single or a progression of lognormal functions. The band maxima given in the text and ESI always correspond to the results of the fitted spectra (reproducibility of the fits: ± 1 nm).

S2 1–II and aggregation. Based on the following considerations, aggregation does not seem to be the effect triggering the appearance of type **II** fluorescence in sols and gels doped with **1**. As mentioned in the text, even when saturated, ethanolic solutions of **1** never showed any other bands than the respective corresponding dilute solutions. For **1**, especially the large and flexible crown unit should prevent spontaneous aggregation. Moreover, since the crown unit does only bind to Hg(II) ions[S1]—which are not present under the conditions used here—cation-assisted dimerization via the crown units sandwiching the metal ion is also very unlikely. Furthermore, the similarity of the spectral data found in the protonation studies (see 3.4.2) disfavor aggregation. This is stressed by a comparison of the red-shifted spectra of **1–II** with those of closely related styryl dyes such as **4**.[S2] Additionally, the occurrence or absence of the red-shifted components in the case of **1** as compared to **2** is well-reflected by their different proton or hydrogen-bonding sensitivities. For π-stacking and aggregation, the exchange of a dimethylamino for a methoxy group is unlikely to have such a dramatic effect.

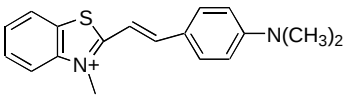

4

A further argument against aggregation is the fact that generally for all the syntheses and both dye concentrations used for **1**, the contribution of bathochromically shifted **II** decreases with increasing storage time as well as with drying immediately after gelation (cf. "G" and "G+M" data in Table 3). However, for dimers or aggregates of other dyes, such a behavior is commonly only found during the aging process of dried gels.[S3] Furthermore, especially the drying/wetting cycles performed with 1_{350}+DY+3_{293} and DY+4_{293} samples, where the relative intensity of **II** positively correlates with the reduced availability of solvent (Table 4), cannot be interpreted as an induction of ordering/disordering phenomena, yielding an (controlled, since the shifts in band positions are negligible) association/dissociation of aggregates. Finally, the bandshape of **1–II** is more reminiscent of an increased ICT process.[S2]

Table S1. Gelation time t_{gel} in days for various sol syntheses and aging temperatures.

Synthesis	N [a]	310 K	296 K	290 K
10_{350}+DY	4	– [b]	28 ± 0	58 ± 1
4_{350}+DY	11	24 ± 0	89 ± 1	132 ± 2
4_{350*} [c]	1	–	–	76
DY+4_{293}	4	26 ± 0	96 ± 3	140 ± 5
1_{350}+DY+3_{293}	6	28 ± 0	99 ± 2	151 ± 3

[a] Number of repetitions. [b] No experiment. [c] 3 h hydrolysis at 350 K.

Table S2. Selected spectroscopic data of **1**-doped gels prior to and during the drying/wetting cycles.

[a]	1_{350}+DY+3_{293}		DY+4_{293}		4_{350}+DY	
	λ_{exc} [b] /nm	λ_{em} [b] /nm	λ_{exc} [b] /nm	λ_{em} [b] /nm	λ_{exc} [b] /nm	λ_{em} [b] /nm
G	412	502	398	495	397	500
G+W	405	493	401	491	404	499
G+W+M	368	474	379	485	376	472
G+W+M+H_2O	391	482	381	485	374	488
G+W+M+H_2O+S	370	496	370	492	370	492
G+W+M+H_2O+S+EtOH	389	494	375	488	375	489

[a] G: gel aged at 310 K, W: wet-aging at 310K, M: drying, H_2O: soaking in water, S: free storage in air at 293 K for 29 d, EtOH: soaking in ethanol. [b] Maxima of fluorescence excitation and emission bands.

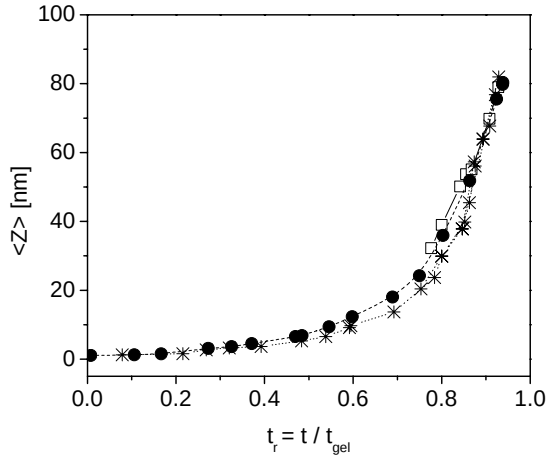

Figure S1. Influence of the synthesis temperature and time during preparation of silica sols on the evolution of the most frequent particle size <Z> during sol aging: sols 4_{350*} (□; synthesis: 3 h at 350 K), 4_{350}+DY (●; synthesis: 2 h at 350 K) and DY+4_{293} (∗; synthesis; 2 h at 293 K). Aging at 290 K. Detection angle 90°. The lines are only guides to the eye.

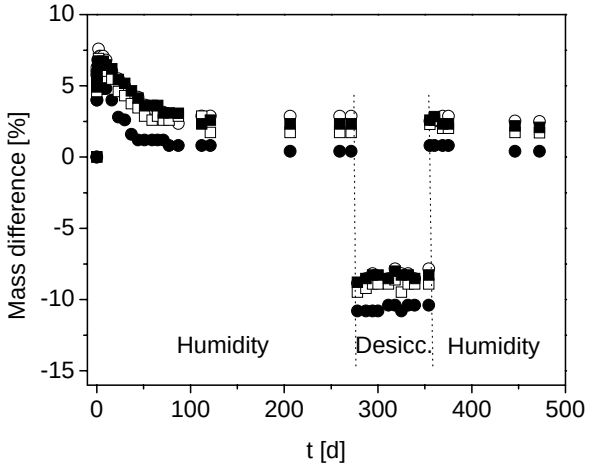

Figure S2. Relative change of sample mass Δ*m* of bulk gels, dried according to procedure "H", during exposure to humid and dry air. Sol 4_{350}+DY aged at 290 K (○) and 310 K (●), Sol 1_{350}+DY+3_{293} aged at 290 K (□) and 310 K (■).

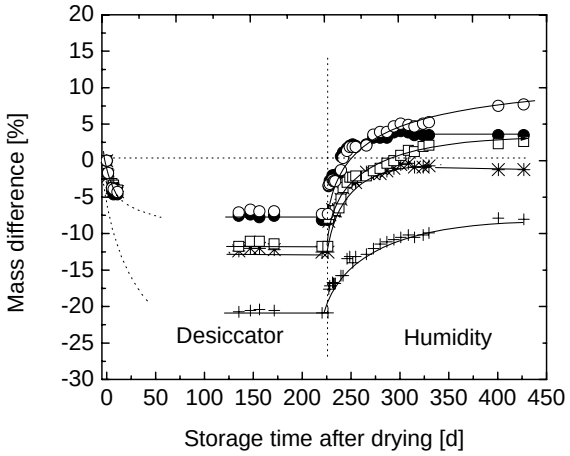

Figure S3. Relative change of sample mass Δ*m* of "M"-dried bulk gels during desiccator storage at 295 K and later storage in humid air (ca. 99 %) at ca. 295 K; sols 4_{350}+DY (●/○, 310/290 K), DY+4_{293} (∗/+, 310/290 K), 1_{350}+DY+3_{293} (□, 290 K). After ~ 70 d, each sample was shortly (3 h) exposed to laboratory atmosphere during spectroscopic measurements.

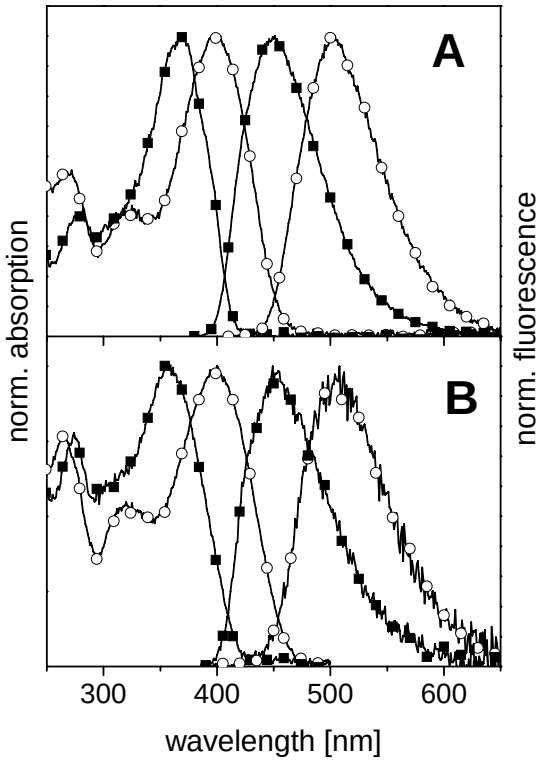

Figure S4. Absorption and fluorescence spectra of **1** (open circles) and **2** (solid squares) in acetonitrile (A) and ethanol (B) solution at 296 K.

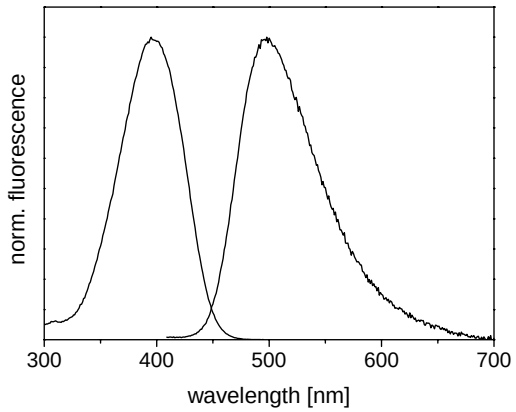

Figure S5. Normalized fluorescence excitation and emission spectra of **3** (10^{-6} M) after hydrolysis on the day of sol synthesis according to procedure 4_{350}+DY, observed at 505 and excited at 350 nm.

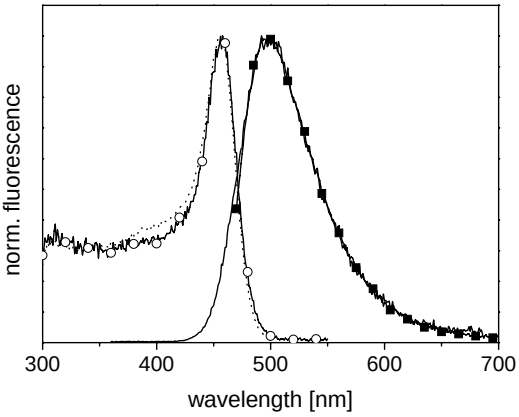

Figure S6. Normalized fluorescence excitation and emission spectra of **3** (10^{-3} M) in a 4_{350}+DY-synthesized monolith, "M"-dried after gelation (290 K) and "R"-dried after an intermediate storage for 4 months at 290 K in a dessicator; observed at 505 (dotted line) and 560 nm (open circles) and excited at 350 (solid line) and 460 nm (solid squares).

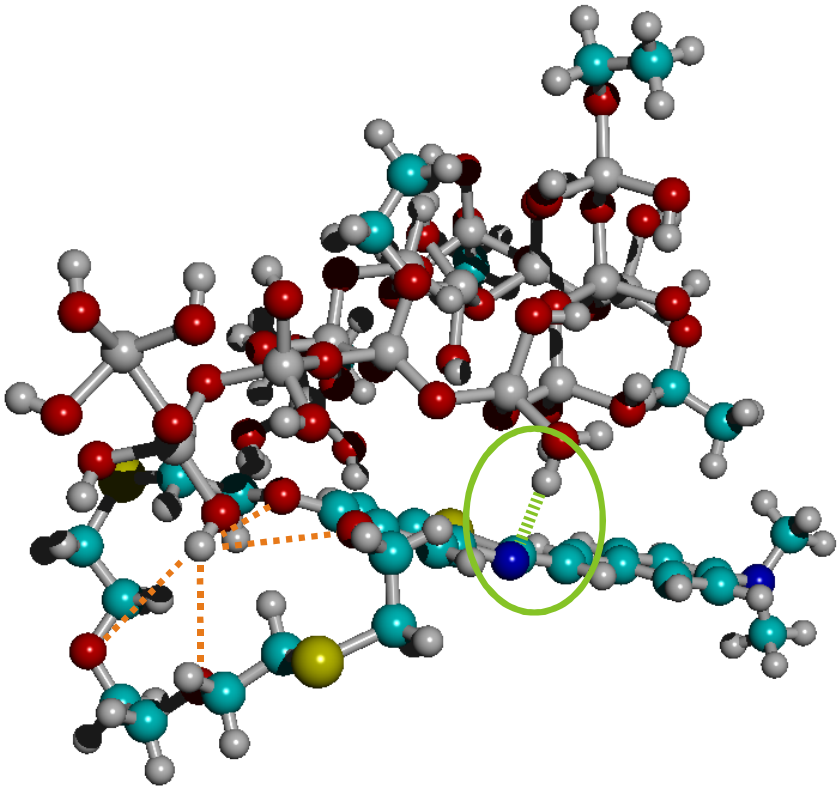

Figure S7. Schematic representation of hydrogen bond-assisted (orange dots) tight interaction (green circle) of a protonated primary particle and the acceptor group nitrogen atom, assumed to be responsible for type **II** fluorescence of **1** (based on a MM+-optimized geometry). Cyan – carbon, red – oxygen, dark blue – nitrogen, yellow – sulfur, grey with four bonds – silicon, grey with one bond – hydrogen atoms.

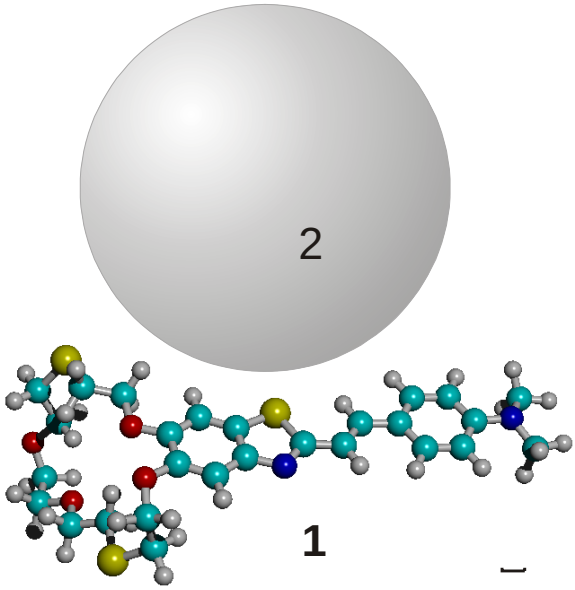

Figure S8. Size relation between dye **1** and a primary SiO_2 sol–gel particle 2 (∅≈ 1–2 nm, > 2 nm during later synthesis stages); bar = 0.1 nm.

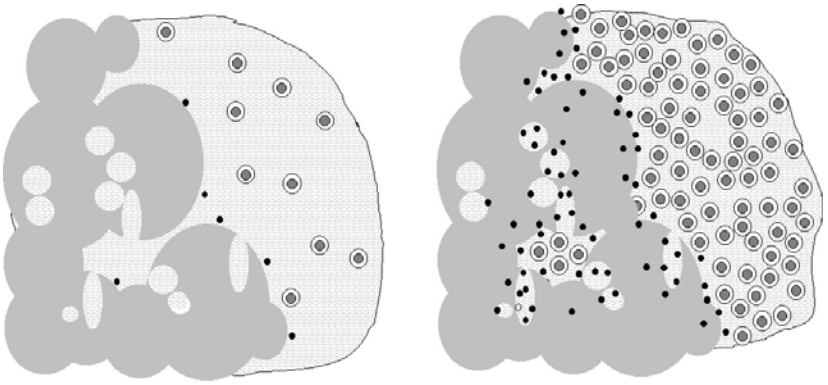

Figure S9. Schematic representation of the effect of dye concentration on the ratio of solvated (species **I**) and adsorbed (species **II**) dye molecules (for key, see Figure 7).

References

S1 W. Rettig, K. Rurack and M. Sczepan, in *New Trends in Fluorescence Spectroscopy: Applications to Chemical and Life Sciences*, B. Valeur and J. C. Brochon, eds., Springer, Berlin, 2001, p. 125.

S2 M. Mitewa, N. Mateeva, L. Antonov and T. Deligeorgiev, *Dyes Pigm.*, 1995, **27**, 219; L. Antonov and M. Mateeva, *Talanta*, 1994, ***41***, 1489; J. L. Bricks, J. L. Slominskii, M. A. Kudinova, A. I. Tolmachev, K. Rurack, U. Resch-Genger and W. Rettig, *J. Photochem. Photobiol., A Chem.*, 2000, **132**, 193.

S3 D. Avnir, D. Levy and R. Reisfeld, *J. Chem. Phys.*, 1984, **88**, 5956; K. K. Flora, M. A. Dabrowski, S. P. Musson and J. D. Brennan, *Can. J. Chem.*, 1999, **77**, 1617.